Integrated patient network and genomic plasmid analysis reveal a regional, multi-species outbreak of carbapenemase-producing Enterobacterales carrying both *bla*$_{IMP}$ and *mcr-9* genes

Adhiratha Boonyasiri[1,2*], Ashleigh C. Myall[1,3*] , Yu Wan[1*], Frances Bolt[1,4,5], Alice Ledda[6,7], Siddharth Mookerjee[4], Andrea Y. Weiße[8,9], Jane F. Turton[7], Hala Abbas[1,10], Ruta Prakapaite[11], Akshay Sabnis[11], Alireza Abdolrasouli[4], Kenny Malpartida-Cardenas[1,12], Luca Miglietta[1,12], Hugo Donaldson[10], Mark Gilchrist[1,4], Katie L. Hopkins[1,7], Matthew J Ellington[1,13], Jonathan A. Otter[1], Gerald Larrouy-Maumus[1,14], Andrew M. Edwards[11], Jesus Rodriguez-Manzano[1,5,12], Xavier Didelot[15], Mauricio Barahona[3], Alison H. Holmes[1,4,5], Elita Jauneikaite[1,6#] and Frances Davies[1,4,10#]

1. NIHR Health Protection Research Unit in Healthcare Associated Infections and Antimicrobial Resistance, Department of Infectious Disease, Imperial College London, Hammersmith Hospital, London, UK.
2. Faculty of Medicine Siriraj Hospital, Mahidol University, Bangkok, Thailand.
3. Department of Mathematics, Imperial College London, London, UK
4. Imperial College Healthcare NHS Trust, London, UK
5. Centre for Antimicrobial Optimisation, Hammersmith Hospital, Imperial College London, Du Cane Road, London, UK
6. Department of Infectious Disease Epidemiology, School of Public Health, Imperial College London, London, UK
7. HCAI, Fungal, AMR, AMU & Sepsis Division, UK Health Security Agency, London, UK
8. School of Biological Sciences, University of Edinburgh, Scotland, UK
9. School of Informatics, University of Edinburgh, Scotland, UK
10. Department of Microbiology, North West London Pathology, London, UK
11. MRC Centre for Molecular Bacteriology and Infection, Department of Infectious Disease, Faculty of Medicine, Imperial College London, London, United Kingdom
12. Centre for Bio-Inspired Technology, Department of Electrical and Electronic Engineering, Faculty of Engineering, Imperial College London, UK
13. Reference Services Division, UK Health Security Agency, London, UK
14. MRC Centre for Molecular Bacteriology and Infection, Department of Life Sciences, Faculty of Natural Sciences, Imperial College London, London, UK

15. School of Life Sciences and Department of Statistics, University of Warwick, UK

* These authors contributed equally; # these senior authors contributed equally.

Keywords: Carbapenem-resistant Enterobacterales, IMP carbapenemase, antimicrobial resistance, horizontal gene transfer, molecular epidemiology, spatiotemporal network, patient pathways

Abstract

The incidence of carbapenemase-producing Enterobacterales (CPE) is rising globally, yet Imipenemase (IMP) carbapenemases remain relatively rare. This study describes an investigation of the emergence of IMP-encoding CPE amongst diverse Enterobacterales species between 2016 and 2019 in patients across a London regional hospital network.

A network analysis approach to patient pathways, using routinely collected electronic health records, identified previously unrecognised contacts between patients who were IMP CPE positive on screening, implying potential bacterial transmission events. Whole genome sequencing of 85 Enterobacterales isolates from these patients revealed that 86% (73/85) were diverse species (predominantly *Klebsiella* spp, *Enterobacter* spp, *E. coli*) and harboured an IncHI2 plasmid, which carried both bla_{IMP} and the putative mobile colistin resistance gene *mcr-9*. Detailed phylogenetic analysis identified two distinct IncHI2 plasmid lineages, A and B, both of which showed significant association with patient movements between four hospital sites and across medical specialities.

Combined, our patient network and plasmid analyses demonstrate an interspecies, plasmid-mediated outbreak of bla_{IMP}CPE, which remained unidentified during standard microbiology and infection control investigations. With whole genome sequencing (WGS) technologies and large-data incorporation, the outbreak investigation approach proposed here provides a framework for real-time identification of key factors causing pathogen spread. Analysing outbreaks at the plasmid level reveals that resistance may be wider spread than suspected, allowing more targetted interventions to stop the transmission of resistance within hospital networks.

Introduction

Infections by carbapenemase-producing Enterobacterales (CPE) pose a substantial clinical, operational, and financial challenge[1]. These organisms are associated with high morbidity and mortality, and therapeutic options are severely restricted[2,3]. Carbapenemase genes are frequently carried on plasmids, which can easily transfer between bacterial species. CPE outbreaks involving different bacterial species are often unrecognised, as many plasmids are variable in their gene content[4] and have a broad host range[5]. The metallo-β-lactamase – (MBL) Imipenemase gene (IMP)-1, was first described in *Pseudomonas aeruginosa*[6], whilst IMP genes have spread globally, outbreaks in Enterobacterales species are mostly sporadic and often localised to specific geographical locations[7-9]. IMP genes are rarely isolated in the UK, but the number of IMP encoding isolates within Enterobacterales species referred to UK Health Security Agency (UK HSA) has been increasing[10,11].

Therapeutic options are particularly limited for MBL CPEs, with limited efficacy of the newer beta-lactam combination agents[2,3]. Colistin and polymyxin B remain the last-line therapeutic agents in most countries, partly due to lack of access to newer agents; yet resistance is increasing globally, particularly through mobilised colistin resistance (*mcr*) genes on plasmids[12,13]. Since the first discovery of *mcr*-1 in 2016[14], ten *mcr* genes (*mcr*-1 to *mcr*-10) have been described to date, presenting a substantial global healthcare challenge[13,15]. Although *mcr* genes are typically associated with phenotypic polymyxin resistance, *mcr-9*, identified in 2019, does not appear to confer direct colistin resistance[7,16]. It has been detected in clinical isolates co-harbouring different resistance genes in Australia (with $bla_{\text{IMP-4}}$), South Africa (with ESBLs), Egypt and the Netherlands (with bla_{VIM}) and Japan (with $bla_{\text{IMP-1}}$)[7,8,17-20], and is widespread in isolates from human, animal and environmental origins, in a wide range of bacterial species[7,21].

Person-to-person contact is a route of transmission for many infectious diseases. Consequently, understanding the patterns of these contacts, especially in healthcare settings, can offer detailed insight for targeted interventions[22]. Contact patterns, however, become increasingly complex when considering large numbers of interacting individuals over long-time spans, bacterial interactions with the human host and environment, bacterial behaviour under antibiotic and disinfectant pressure, and plasmids that can be shared by multiple bacterial species. Network models provide flexible tools to capture such complex contact patterns,with the availability of

100 well-developed analytical toolboxes they offer robust and reproducible methodology that has
101 become widespread across disciplines[23]. Network models of infectious diseases[24-26] incorporate
102 both person-to-person transmission through contact networks[27-30] and spatial spread through
103 networks representing physical locations and their relationships[31,32]. So far, studies utlising
104 network models of patient contacts in combination with detailed genomic analysis of bacterial
105 isolates have demonstrated their promise through increasing the detail in outbreak
106 characterisation [33,34].
107
108 Here we describe the emergence of *bla*$_{IMP}$ and *mcr-9* co-harboured by diverse Enterobacterales
109 species that have been isolated from patients across a regional network of London hospitals
110 between 2016 and 2019. We combine in-depth phylogenomic analysis of the IncHI2 plasmid
111 containing *mcr-9* and *bla*$_{IMP}$ with a network model of patient movements to provide novel
112 insight into the spread and dissemination of *bla*$_{IMP}$ and *mcr-9* between bacterial species and
113 patients over 3 years, with implications for how CPE clusters are identified and managed in the
114 hospital setting.
115
116
117 **Results**
118 ***Emergence of bla*$_{IMP}$CPE**
119 Following the introduction of enhanced CPE screening in 2015[35], a CPE-carrying *bla*$_{IMP}$
120 (*bla*$_{IMP}$CPE) was first observed in our hospital group in June 2016 from a routine rectal
121 screening sample. From November 2016, increasing numbers of *bla*$_{IMP}$CPE isolates were
122 identified across diverse Enterobacterales species at three of the acute hospital sites
123 (representing 64% of all inpatient beds at our institution) (**Figure 1a**), and simultaneously at
124 two other external hospitals in the regional network, all served by the same microbiology
125 diagnostics laboratory, and closely connected by regular inter-hospital patient transfers. The
126 highest incidence of *bla*$_{IMP}$CPE cases occurred in January and April 2019 (**Figure 1b**). In total,
127 *bla*$_{IMP}$CPE were isolated from screening or clinical samples from 116 patients who were
128 admitted to our hospital group up until the end of November 2019, when new cases rapidly
129 dropped, despite no targeted changes in infection control interventions. However, only two
130 clusters of cases, (totalling 5 out of 116 cases), fitted the real-time infection control outbreak
131 definition, i.e. two or more cases of the same bacterial species with the same resistance
132 mechanism overlapping in time and space. Pulsed Field Gel Electrophoresis (PFGE) typing

133 performed at the public health laboratories for those 5 cases had confirmed similarity,
134 suggesting cross transmission events had occured.
135 To reveal the operational burden of *bla*$_{IMP}$CPE, the daily number of occupied beds was
136 computed for all colonised patients. The analysis revealed a continuous burden of patients
137 colonised with *bla*$_{IMP}$CPE which was far higher than expected from the new case incidence,
138 particularly for those colonised with *Enterobacter* species (**Figure 1a,b**), with 424 total
139 inpatient bed days per month at the peak (March 2019), across the hospital network (**Figure**
140 **1c)**.
141
142 **Figure 1: Characteristics of confirmed *bla*$_{IMP}$CPE patient cases and distribution of CPE**
143 **species. (A)** Total number of days patients (rows labelled by CPE isolate identifier) were
144 present in a hospital ward before confirmed to be colonised/infected with *bla*$_{IMP}$CPE (*in-*
145 *hospital infectious period*) and infection prevention and control measures were taken.
146 Additionally, patients with known carriage of *bla*$_{IMP}$CPE but without sequenced isolates are
147 shown as unlabelled rows. Patients with paired isolates (IMP 22/24, IMP 25/33, IMP 96/97,
148 IMP 100/101) are on adjacent rows. **(B)** Monthly total number of confirmed *bla*$_{IMP}$CPE isolates
149 detected in patients during the study period from 2016 to 2019. **(C)** Weekly cumulative number
150 of bed days of patients with confirmed carriage of *bla*$_{IMP}$CPE before they identified as
151 colonised with *bla*$_{IMP}$CPE over their infectious in-hospital period. Colours in each of the panels
152 indicate the genus of CPE identified in the study.
153

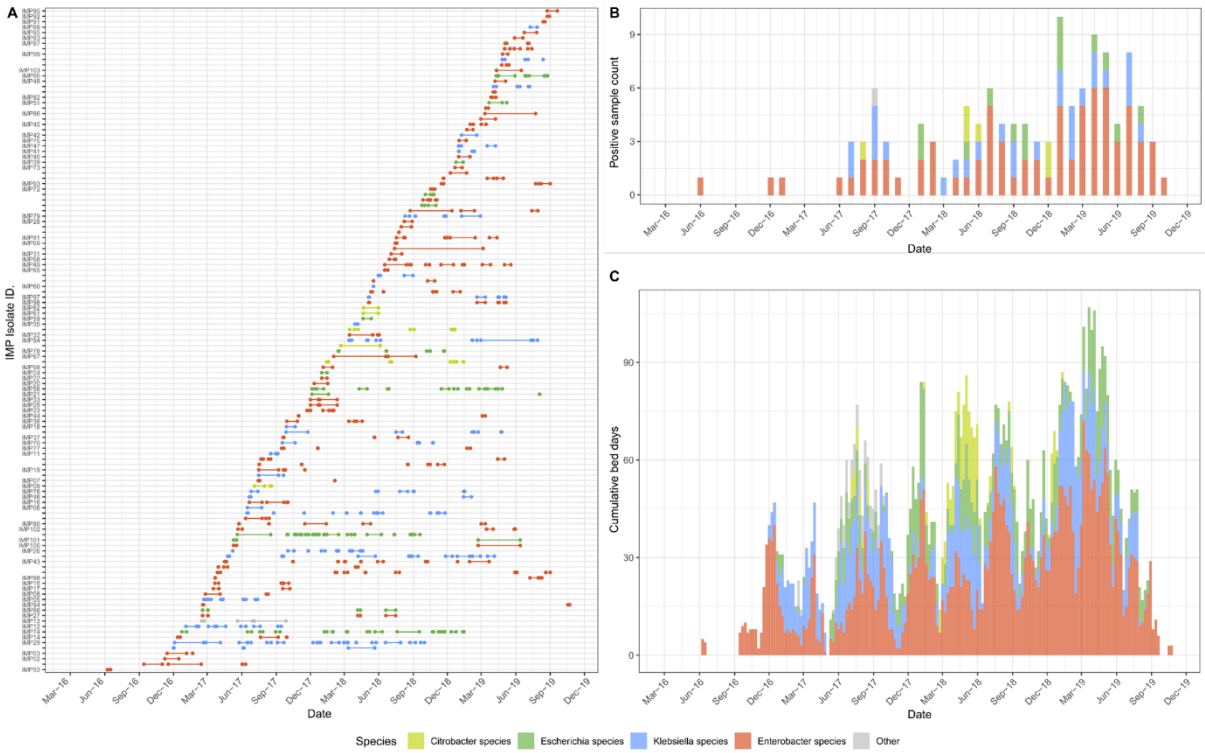

Contact network of bla*$_{IMP}$CPE *patients

A detailed patient contact network for all 116 *bla*$_{IMP}$CPE colonised/infected patients who were identified in our hospital group, including data from their admissions at the other regional hospitals, confirmed that 77/116 (66%) patients were in contact with at least one other *bla*$_{IMP}$CPE colonised/infected patient (**Figure 2**). The analysis showed that the median number of contacts was two per patient, however, contact numbers displayed substantial variation. For example, one patient (Case 85, cluster 1.5) had 10 contacts with 9 other patients which linked them to 8% of all cases (**Table S1**) and therefore identified the patient as a potential 'super-spreader' in the outbreak.

Across all *bla*$_{IMP}$CPE patient contact pairs, 57/96 (59%) pairs differed in bacterial species (8 species identified carrying *bla*$_{IMP}$), explaining why these contacts were not identified as outbreak-related using the clinical infection control outbreak definition, which was reliant on the same bacterial species rather than resistance mechanism. The network of patient contacts split patients into 12 separate clusters, with interactions occurring across hospitals, as patients were transferred between wards and sites **(Figure 2)**. The largest cluster (Cluster 1) contained 45 patients and was partitioned into a further seven subclusters, labelled 1.1 to 1.7, that comprised 13, 12, 2, 6, 5, 5 and 2 patients, respectively (**Figure 2**). The analysis of *bla*$_{IMP}$CPE patient contacts, at regional, individual hospital and ward level, suggested that different species

174 of *bla*$_{IMP}$CPE were involved intransmission events (**Figure 2**). This multi-species involvement
175 in the ongoing outbreak prompted genomic analysis of the available *bla*$_{IMP}$CPE isolates.
176
177 **Figure 2. Patient contact network of interactions among *bla*$_{IMP}$CPE positive patients.**
178 Each node of the network represents a patient (coloured according to *bla*$_{IMP}$CPE isolate
179 species) and each edge represents a contact between two patients. Edges represent recorded
180 contacts between confirmed *bla*$_{IMP}$CPE cases (patients present on the same ward on the same
181 day according to their electronic health records). The patient contact network identified 12
182 distinct clusters (each shaded in a different colour) based on disconnected components of
183 patient contact. Cluster 1, the largest cluster consisting of 45 patients, was further partitioned
184 into 7 subclusters using community detection with edges weighted by duration of contact (see
185 Supplementary methods – Community detection). Six patient contacts re-occurred over
186 different wards, indicated by additional edges connecting the same patients.
187

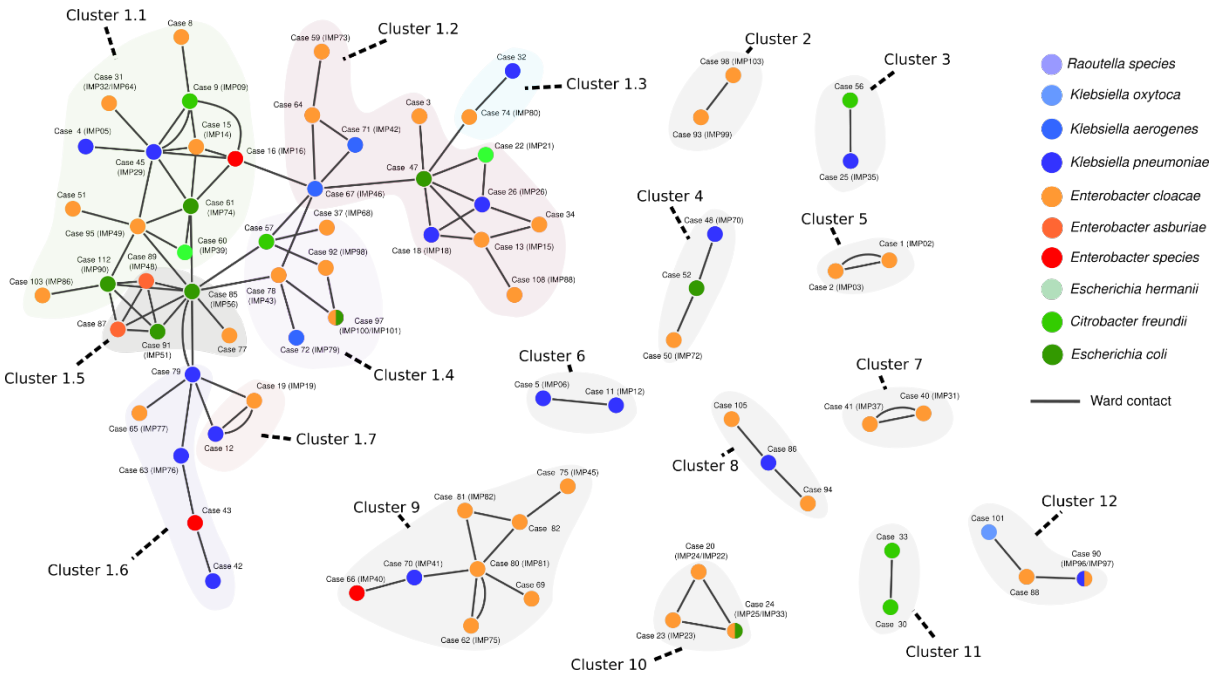

188
189
190 ***Genomic and phenotypic characterisation of bla*$_{IMP}$*CPE isolates***
191 A total of 85 bacterial isolates from 82/116 *bla*$_{IMP}$CPE colonised patients were sequenced for
192 genomic analysis (**Table S2**). The *bla*$_{IMP}$ gene was detected in 13 different bacterial species,
193 most commonly in members of the *Enterobacter cloacae* complex species (55/85), *K.*
194 *pneumoniae* (16/85) and *E. coli* (10/85) (**Table S2**). Most patients harbourd only one *bla*$_{IMP}$

195 encoding species, but there were four patients who were colonised with two different bacterial
196 species that carried *bla*$_{IMP}$ (**Table S2**).
197
198 Genomic analysis identified that two alleles, *bla*$_{IMP-1}$ (75/85) and *bla*$_{IMP-4}$ (10/85), co-occurred
199 with two groups of plasmids: IncHI2 plasmid was identified in 72/85 isolates and IncN3 in
200 11/85 (**Figure 3**). One isolate of *K. aerogenes* (IMP79) carried both plasmids, and two isolates
201 (IMP47, IMP76) carried a different plasmid co-occurring with *bla*$_{IMP-1}$. As expected, all
202 *bla*$_{IMP}$CPE isolates had carried multiple β-lactam resistance genes in addition to other
203 antimicrobial resistance genes (**Table S3**), though only one isolate (IMP89) had another
204 carbapenem resistance gene, *bla*$_{OXA-48}$ (**Table S3**).
205
206 **Figure 3. Phylogenetic tree of 85 Enterobacterales genomes in this study.** A neighbour-
207 joining phylogenetic tree of 85 Enterobacterales genomes was constructed using whole-
208 genome FastANI distances. The colour at the end of each branch indicates the species identity
209 for that isolate. The rings are as follows: the innermost ring indicates the type of plasmid
210 detected; the middle ring indicates the allelic variant of the *bla*$_{IMP}$ gene detected, and the outer
211 ring indicates the presence or absence of the *mcr-9* gene. NF = not found. The scale bar
212 indicates the average nucleotide distance (in percent) per site.

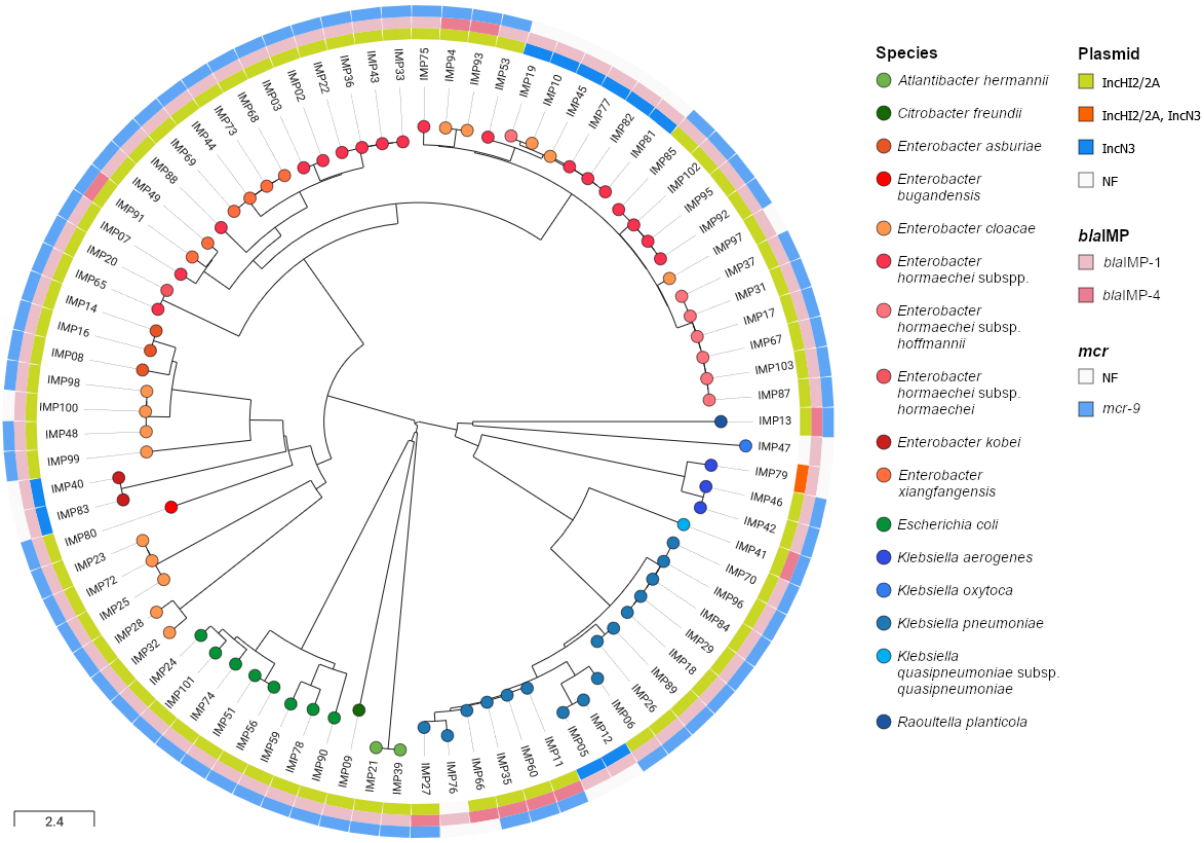

213

214

215 The multi-species distribution of the 72 IncHI2 plasmids among contact network linked
216 patients, was highly suggestive of plasmid mobility. The *mcr*-9 gene was detected in 81%
217 (69/85) of all bla_{IMP}CPE isolates, all of which harboured the IncHI2 plasmid (94% 69/72 of
218 IncHI2 plasmid carrying isolates; none of IncN3 plasmids had *mcr-9*). The *mcr*-9 specific
219 LAMP assay confirmed the presence of *mcr-9* with 100% concordance (**Table S4**) as
220 previously reported[36]. MALDIxin (which detects modifications to the lipid A of the
221 lipopolysaccharide as mediated by *mcr*1-5 and *mcr*-8[37]) did not detect any Lipid A
222 modifications attributable to the *mcr*-9 gene in this study. Altogether, 12/84 isolates tested (all
223 *Enterobacter* species) were resistant to colistin with MICs > 2 µg/ml (range 4 to >64 µg/ml)
224 (**Table S4**), and 5 isolates demonstrated a skipped-well phenomenon[38] suggestive of colistin
225 heteroresistance. However, determining the contribution of *mcr-9* or other mechanisms of
226 resistance to this was beyond the scope of this study, and will be the subject of future
227 investigations.

228

229 ***Population structure of IncHI2 plasmids***

230 Phylogenetic analysis of the 72 IncHI2 plasmids (where reads were mapped to complete
231 genomic sequence of plasmid pKA_P10 (NZ_CP044215.1)) identified two major lineages (A
232 and B) and four sublineages (A.1, A.2, B.1 and B.2, **Figure 4**). While all the isolates were
233 carrying multiple antimicrobial resistance (AMR) genes and multiple plasmids, only plasmids
234 of the B.1 lineage carried bla_{IMP-4} and were present in isolates that also exclusively saw co-
235 occurrence of *tet*(D)*, qnrB2,* bla_{OXA-1} and *mph*(A) (**Figure 4**). Comparison of 233 plasmid core-
236 genome single-nucleotide polymorphisms (cgSNPs) showed some congruency of cgSNPs with
237 the plasmid sequences (**Figure S1)**. Furthermore, this analysis grouped the IncHI2 plasmids
238 into 15 polytomic clades (with identical SNP profiles), of which 12 showed identical cgSNPs
239 after masking recombination regions (**Table S5** and **Figure S2**).

240

241 **Figure 4. Dated phylogenetic tree showing the relationship between 72 IncHI2 plasmids**
242 **identified in CPE isolates with** bla_{IMP}**.** The complete genome of IncHI2 plasmid pKA_P10
243 was used as the reference for variant calling. The tree was generated and rooted using
244 BactDating. Branch colours denote major plasmid lineages, which are supported by bootstrap
245 values of 100. At the tips of the tree, circles represent plasmids from routine rectal screening
246 samples, and squares represent plasmids from clinical samples. Colours of the tip symbols
247 indicate species. Lineage identifiers are labelled above lineage-specific root branches. The

column panel to the right of the phylogenetic tree indicates presence-absence of mobile antimicrobial resistance genes and plasmid replicons. NA: information was not available.

The root of the plasmid tree was dated in 1949 (95% CI: 1927-1971), with the most recent common ancestors of lineages A and B dated in 1965 (95% CI: 1943–1988) and 1967 (95% CI: 1945–1988), respectively (**Figure S3**). These estimates suggest that not only IncHI2 plasmids have been circulating amongst *Enterobacterales* for many decades, but also that they have undergone extensive evolution in the antibiotic era.

Plasmid lineages and patient cluster comparisons

To investigate if the identified IncHI2 plasmid lineages A and B were responsible for the emergence of *bla*$_{IMP}$CPE in our hospital network, plasmid genomic data was overlaid onto the

263 patient contact network (**Figure 5, Figure S4).** IncHI2 plasmid lineage A (3/72 IncHI2
264 plasmids) was exclusively linked to patients in cluster 5 (**Figure 5**), with contacts confined to
265 the same hospital site, highly suggestive of a patient-to-patient or common-source transmission
266 event. The predominant IncHI2 plasmid clade B, representing 69/72 plasmids sequenced and
267 60% of all cases identified in the study, was distributed widely across the hospital network,
268 dominated Cluster 1 of patient contact clusters, and showed particularly strong association with
269 contacts at hospital site 3 (**Figure 5**). The IncN3 plasmid (9.5% of overall cases) displayed
270 strong association with patients in network Cluster 9, with contacts occurring at three different
271 hospitals (hospitals 1, 2 and 3) (**Figure 5**). Although 3 of the IncN3 cases in cluster 9 had been
272 identified as an outbreak (Cases 80, 81 and 82) at the time of initial isolate identification, 5
273 other linked cases have now been revealed by this combined network and plasmid analysis,
274 that were previously missed. Similarly, Cases 67 and 71 (Cluster 1.2), identified real-time as
275 related cases, are revealed by this combined analysis to be linked to multiple (n=34) other cases
276 across clusters 1.1, 1.2, 1.3 and 1.4, with the IncHI2 plasmid lineage B.2.
277
278 **Figure 5. Patient contact network of interactions among patients focussed on specific**
279 **locations of contact and plasmid information.** Each node represents a patient, edges
280 represent recorded ward contacts between confirmed *bla*$_{IMP}$CPE cases. The edges are coloured
281 according to the hospital site (site 1-4) and the width of the edge is proportional to the duration
282 of the contact. Cluster nodes are coloured according to the lineage of the IncHI2 plasmid
283 identified in whole genome sequenced *bla*$_{IMP}$CPE isolates; patients with isolates lacking the
284 IncHI2 plasmid are coloured in white; patients with no whole genome sequenced *bla*$_{IMP}$CPE
285 isolates are displayed as labels without a circle. The presence of an IncN3 plasmid in the
286 *bla*$_{IMP}$CPE isolates is denoted by dark-grey borders surrounding the nodes. Contact network
287 clusters are highlighted with individual colour shading as in Figure 4.
288

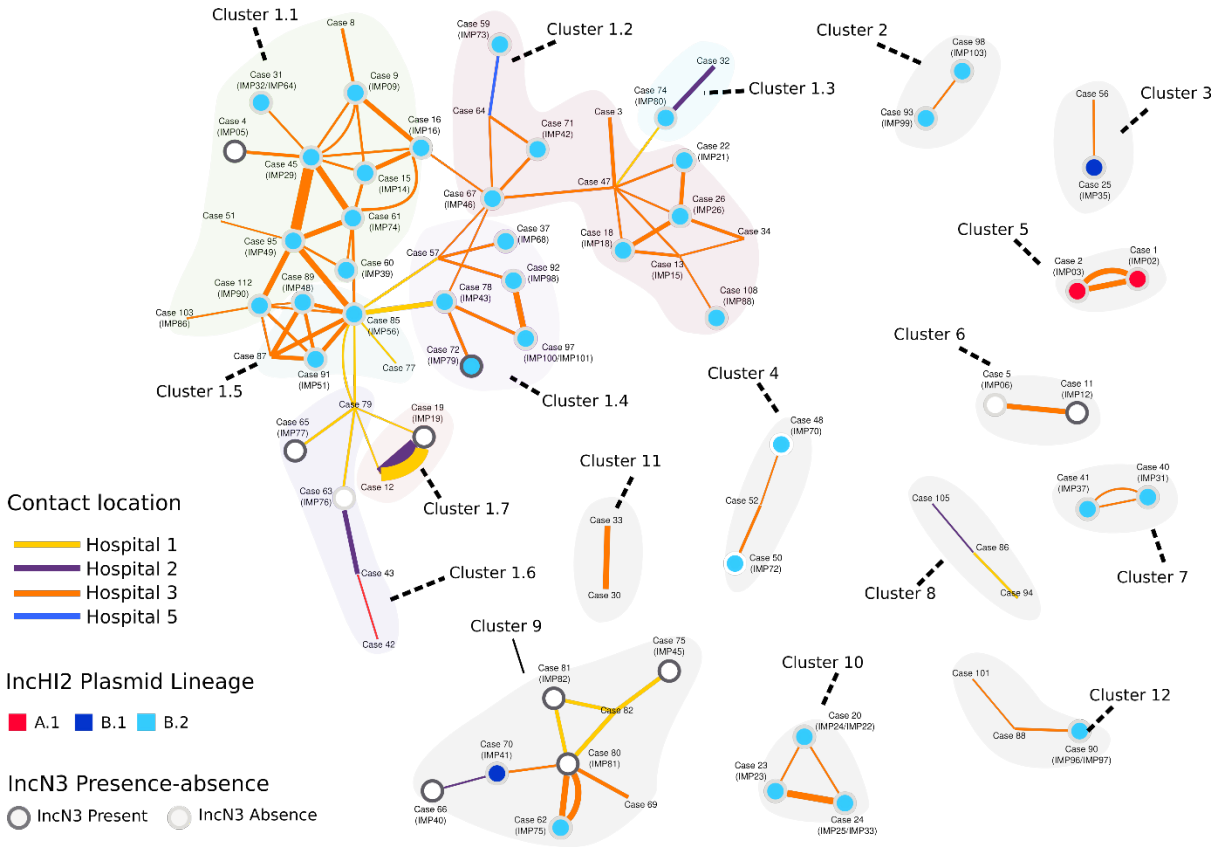

Bacterial sequence data was missing from some cases that could have clarified links between and within plasmid lineages A and B, as suggested by the contact network analysis. Similarly, data was not available for potentially linked cases identified at other regional sites but not transferred to our hospital network. Despite missing hospital network data, clear associations between plasmid clades and patient pathway network clusters are evident, supporting the hypothesis of plasmid spread throughout the course of this outbreak, particularly at hospital 3. When reviewing the cumulative burden of the plasmid clades over time, it becomes apparent that most of the the cumulative bed days of patients shown in Figure 1 are due to patients colonised with clade B2 (**Figure S5**).

Spatial and temporal analysis

Having identified four plasmid lineages among the 72 *bla*$_{IMP}$-CPE IncHI2 plasmids, a network was constructed capturing the structure of patient transfers among hospital wards and used to investigate the spatial distribution of the four major plasmid lineages **(Figure 6).** The smaller plasmid lineages A.1 and A.2 were present in only two and one patients, respectively, and hence, were locally constrained by a smaller set of patient movements. Plasmid lineage A.1 was localised within hospital 3 renal services and had no recorded patient inter-hospital

movement. Plasmid lineage A.2 was localised to a single patient movement within hospital 4, then an inter-hospital movement to hospital 2. Patients with isolates in plasmid lineage B.1 were recorded on wards from hospital sites 1, 2, 3 and 5. However, inter-hospital transfers of these patients were only recorded between hospitals 2 and 5, and hospitals 3 and 5. It is thus likely that some transmission of plasmid lineages B.1 was missed, either through patients who were not detected on screening, or these were patients whose isolates were not available for sequencing. Plasmid lineage B.2 was spatially more distributed with recorded multiple bi-directional inter-hospital transfers among hospital sites 1, 2, 3 and 5. Looking at the association between plasmid lineage clusters and ward/specialties over the study periodthe most common associations across all specialities were critical care and renal services (**Table S6**). The only exception was general internal medicine and general surgery predominated in plasmid lineage B.1 at hospital site 5, which has more general wards and less specialist services than the other hospital sites in the network. Despite the predominance of cases being identified in specialties with high risk for invasive disease, only 4 clinical infections were identified during the study, and no blood stream infections (**Table S2**)

Figure 6. **Spatial analysis representing the pathways of patient transfers among wards and hospitals.** Movement of patients carrying bla_{IMP}CPE are represented by arrows between wards (nodes) and the five hospitals (dotted ovals). For hospital site 5, only hospital-level data was available, therefore, only intra-hospital movement is shown. Repeated transfers of patients between wards are aggregated into edges withproportionally greater edge width. Plasmid clusters, based on plasmid lineage (A.1, A.2, B.1 and B.2) are coloured accordingly. For patients with multiple CPE isolates, transfers are duplicated to match each isolate uniquely in the visualisation.

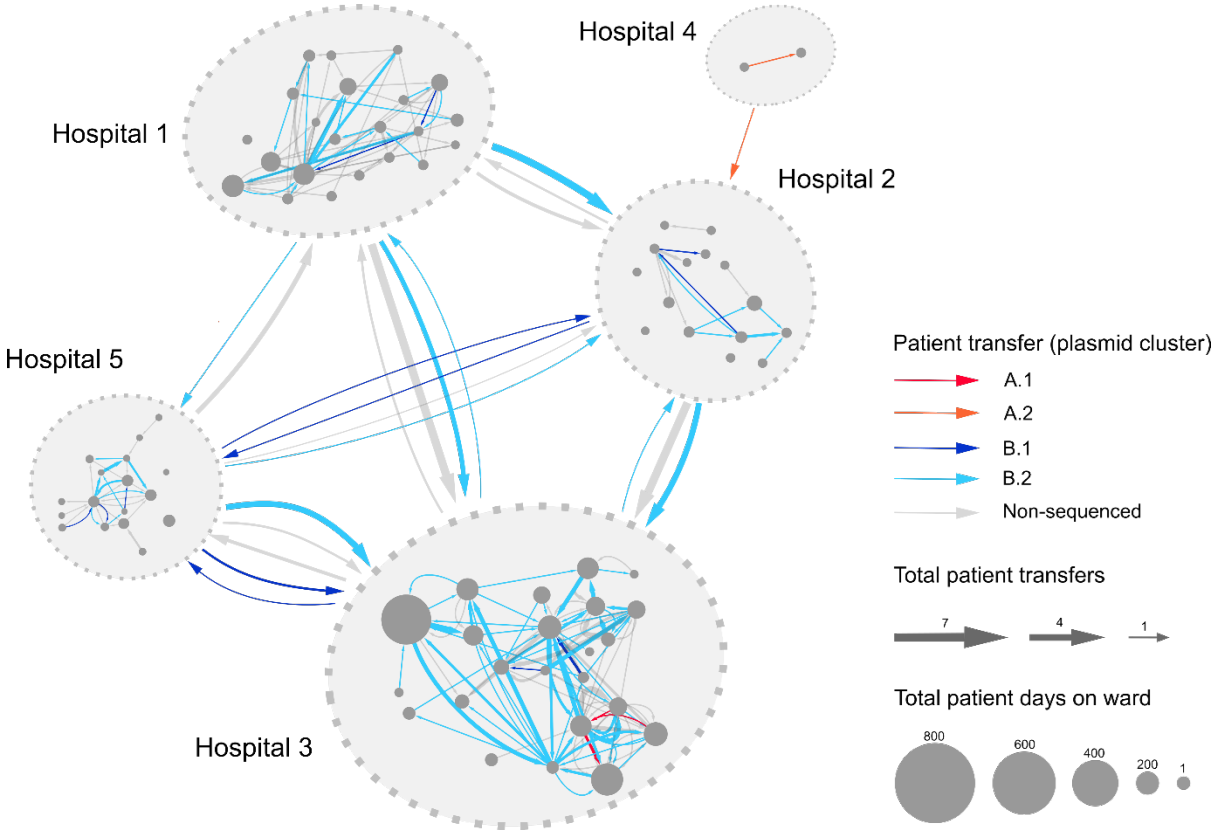

333
334
335 Although the first case was identified in 2016 (IMP 51/Case 91), a temporal network analysis
336 indicated it played only a minor role in onward transmission, due to the small number of
337 reachable patients over time (**Figure S6**). This may suggest that previous/subsequent patients
338 were not identified or point to the existence of an environmental reservoir. Considering the
339 timing and ordering of all contacts, IMP79 could have seeded up to 27 subsequent cases
340 (restricted to those in Cluster 1 in **Figure 2**), either directly or indirectlty, via possible
341 transmission routes. The patient carried the isolate that co-harboured both IncN3 and IncHI2
342 plasmids, potentially suggesting multiple transmission opportunities to, as well as, from, this
343 patient. There were 14 patients (15 isolates) from the 72 isolates carrying an IncHI2 plasmid,
344 which had a proportionately larger number of reachable time-ordered contacts, suggesting that
345 these patients may also have contributed substantially to transmission (**Figure S6**).
346
347 These integrated geno-spatio-temporal representations show that the spread of plasmids
348 containing bla_{IMP} followed patient movements for specialty care around the region, with
349 possibly multiple introductions and re-introductions of the plasmid at different points during
350 the patient journeys, and multiple chances for cross transmission events to have occurred.
351

352

353 **Discussion**

354 Following the detection of a new mechanism of resistance, investigation of its origin and mode
355 of transmission is challenging, especially in healthcare settings where investigations usually
356 focus on single species cross transmissions. With confounding factors such as multiple
357 bacterial species and spread over different hospital locations, new methods to investigate
358 potential outbreaks are much needed. The incorporation of plasmid genomics and patient
359 networks into our analysis changed the way the emergence of *bla*$_{IMP}$CPE was visualised and
360 produced a clearer understanding of the high-risk ward locations and pathways for potential
361 cross transmission in our regional healthcare system. As patients were found to follow common
362 routes, with regular re-encounters, this information can provide dynamic risk assessments to
363 be introduced along those pathways, to prevent future cross transmission events of any
364 healthcare-associated pathogen from occurring[39]. Detailed genomic analysis of plasmids
365 enhanced our understanding of the relatedness of different patient isolates to the network
366 analysis. It moreover revealed concerning information about unsuspected resistance
367 mechanisms, with potential for antibiotic treatment failures that were missed on conventional
368 laboratory susceptibility testing. In this study, we characterized IncHI2 plasmids as the main
369 vehicle in horizontal transfer of the metallo-β-lactamase gene *bla*$_{IMP}$. A dated phylogeny of the
370 IncHI2 plasmid carrying *bla*$_{IMP}$, indicated that this plasmid underwent a clonal expansion
371 around 2008, about 8 years before the onset of the outbreak described in our study. IncHI2
372 plasmids are common, large plasmids with a wide host range, that has been reported globally[19],
373 and more recently have been reported to be associated with colistin resistance genes *mcr*-1 and
374 *mcr*-3[40,41]. Although in our study we detected *mcr-9* in 81% of the isolates tested, we did not
375 find evidence of phenotypic expression of this gene, in line with previous observations[7,42]. We
376 identified the predominant IncHI2 plasmid in multiple different bacterial species across linked
377 patients, highlighting the need for integration of genomics into routine clinical practice.
378 Although this study focussed on the emergence of the *bla*$_{IMP}$ carbapenemase gene in our
379 hospital network, it supports the concept that plasmid analysis across different resistance
380 mechanisms as well as among different species should be the standard for investigations in the
381 future. The small number of clinical infections from this outbreak in comparison to other CPE
382 outbreaks from our hospital network[43] and other reports of *bla*$_{IMP}$ CPE[7,19] is noteworthy, and
383 poses questions about the wider importance of this plasmid and the resistance mechanisms
384 revealed in this study. This observation reinforces the argument that screening for silent
385 carriage of CPE in hospitals is key to preventing spread[44-46], and cautious antimicrobial

386 stewardship is essential to prevent expression of hidden resistance mechanisms[47].The
387 association of IMP carbapenemases and drainage[48,49], leads to speculation that the acquisition
388 of this plasmid may provide an environmental survival advantage, enhancing the potential for
389 spread between human hosts through a poorly maintained plumbing environment[50,51].
390
391 We acknowledge some limitations of our study. Firstly, long-read data was available only for
392 two isolates, pKA_P10 and pEB_P9 (NZ_CP043767.1)[10] , and though both were tested as
393 references, assumptions had to be made for in-depth genomic analysis of our plasmids. As a
394 result, our plasmid tree may omit some similarities and differences between identified IncHI2
395 plasmids. Secondly, full pathway data across the hospital during the three years of the outbreak
396 was only available for identified positive cases, not for all patients. It was therefore not possible
397 to fully establish potential missed cases flagging as close contacts but with potential for missed
398 screening or false negative results. Full pathway movement data for all positive cases identified
399 within our hospital network was available, yet neither pathway details nor genomic data were
400 available for other *bla*$_{IMP}$CPE-positive cases identified in the two other regional hospitals who
401 did not visit our institution, thus reducing the understanding in our analysis. Interactions at
402 other potential hospital locations such as interventional imaging or endoscopy were not
403 examined in this study, nor was environmental sampling performed, which could inform future
404 studies on modes of transmission. Nevertheless, this study highlights a previously unidentified
405 extent of transmission and thus provides valuable new insights into the spread of an emerging
406 resistance mechanism. Moreover, our novel multi-layered methodology, incorporating plasmid
407 phylogeny with contact network analysis, provides invaluable tools for outbreak investigation
408 that can be generalised to a wide range of scenarios.
409
410

411 **Materials and Methods**

412 *Clinical Setting*

413 This study was carried out using data from a regional network of London hospitals, comprising
414 of 7 hospital sites with a total of 2000 inpatient beds, with managerial responsibility assigned
415 to 2 different NHS Trusts. Cases of colonisation/infection with *bla*$_{IMP}$CPE were identified at 3
416 hospital sites from one NHS trust (referred to as our Institution in the results) and 2 hospital
417 sites from the other. All hospitals in the network are are served by the same centralised

418 microbiology laboratory and patients are frequently transferred between hospitals in the
419 regional network for specialist investigations and treatment.
420
421 *Sampling, microbiology, antimicrobial susceptibility testing and detection of mcr-9*
422 *bla*$_{IMP}$-encoding Enterobacterales isolates were cultured from rectal screens or clinical samples
423 as part of routine diagnostic testing between June 2016 and November 2019. Rectal screens
424 were cultured on chromogenic media (Colorex™ mSuperCARBA™, E&O Laboratories, UK),
425 and species identification was performed using Biotyper MALDI-TOF MS (Bruker Daltonics,
426 Germany) according to the manufacturer's protocol. Antimicrobial susceptibility testing was
427 performed according to EUCAST guidelines [52], colistin susceptibility testing was performed
428 by broth microdilution on all viable isolates according to manufacturer's instructions
429 (MICRONAUT, BioConnections, UK) [52] . The identification and detection of carbapenemase
430 genes was by PCR (Xpert® Carba-R, Cepheid Inc, USA). After February 2018, all isolates were
431 tested using the RESIST 3 O.K.N. K.SeT (Coris BioConcept, Belgium), and negative isolates
432 had the carbapenem inactivation method (CIM) performed, and CIM positive isolates then had
433 PCR (Xpert® Carba-R, Cepheid Inc, USA) performed as previously described[35]. *bla*$_{IMP}$ positive
434 isolates with suspected links were sent to UK Health Security Agency (UK HSA) reference
435 laboratories for typing by Variable Number Tandem Repeat VNTR (*Klebsiella* sp.) or Pulsed
436 Field Gel Electrophoresis PFGE (all other species).
437 Loop-mediated isothermal amplification (LAMP) was used to examine the prevalence of *mcr-*
438 *9* amongst *bla*$_{IMP}$CPE isolates as described previously [53]. MALDIxin testing was conducted to
439 confirm phenotypic colistin resistance, as previously described on isolates IMP 1-58 only[37].
440
441 *Whole-genome sequencing*
442 Bacterial isolates were grown on Columbia Blood Agar (Oxoid Ltd, UK), incubated aerobically
443 at 37°C overnight before DNA extraction. Genomic DNA was extracted using GenElute™
444 Bacterial Genomic DNA Kit (Sigma-Aldrich, USA) following manufacturer instructions.
445 Multiplexed DNA libraries were generated with Nextera XT (Illumina, USA) and were
446 sequenced for a minimum of 100-fold average coverage on Illumina HiSeq 4000 systems under
447 a 150-bp paired-end layout. Seven isolates (IMP09/CB_P14_L5_12.18,
448 IMP29/KP_P12_L5_11.18, IMP33/EB_P9_L5_03.19, IMP40/EB_P8_L5_01.19,
449 IMP41/KQ_P11_L5_04.19, IMP42/KA_P10_L5_03.19, IMP45/ EB_P13_L5_04.19) were
450 also sent to UK HSA for MinION (Oxford Nanopore, UK) long-read sequencing [10].
451

452 *Sequence data processing and analyses*

453 Short-read sequence reads were quality assessed using FastQC v0.11.6 [54]. Raw reads were
454 trimmed using Trimmomatic v0.39[55] and were *de novo* assembled using SPAdes v3.11 [56] and
455 annotated with Prokka [57]. Species identification was confirmed with KmerFinder 3.2 [58].
456 Multilocus sequence typing (MLST) was performed with the MLST v1.8 online server [59] using
457 the Achtman MLST scheme for *E. coli* curated on PubMLST and EnteroBase[60] and the Pasteur
458 MLST scheme for other *Enterobacterales* isolates. AMR genes, and plasmid typing (**Table S7**)
459 were done using ResFinder v3.2 [61], and PlasmidFinder v2.1 [62], respectively. A neighbour-
460 joining tree of CPE isolates used in this study was generated from assemblies using FastANI
461 v1.3 based on whole-genome average nucleotide identities [63].

462

463 *Phylogenetic analysis of IncHI2 plasmids*

464 A reference complete genome of IncHI2 plasmids was selected from three candidates:
465 pKA_P10 (NZ_CP044215.1; 334 kbp) from *Klebsiella aerogenes*, pEB_P9 (NZ_CP043767.1;
466 331 kbp) from *Enterobacter hormaechei* isolate[10] and R478 (NC_005211.1; 275 kbp)
467 identified in *Serratia marcescens*[64]. The selection aimed to maximise: (i) overall coverage of
468 each reference genome by reads, (ii) the number of plasmid core-genome SNPs identified from
469 the read alignment, and (iii) bootstrap values supporting major lineages in the plasmid
470 phylogenetic tree reconstructed using the same approach based on each reference. Eventually,
471 plasmid pKA_P10 was determined as the reference for the rest of analysis (**Figures S7**).

472

473 Repetitive regions (≥90% nucleotide identity) in the reference plasmid genome were identified
474 using NUCmer of MUMer v3.1[65]. Processed short reads of 73 IMP isolates harbouring IncHI2
475 plasmids were further filtered for a minimum length of 50 bp using Trimmomatic for improving
476 mapping specificity, given estimated read depths >100 fold per bacterial genome before and
477 after the filtering. Filtered reads were mapped to the reference pKA_P10 using Snippy
478 (github.com/tseemann/snippy) with parameters set to as follows: mapping quality ≥ Q60, base
479 quality ≥ Q20, base coverage ≥10 folds, and variant-call quality ≥ Q100. Plasmid pIMP06 was
480 excluded from further steps as its reads covered only 27% of the reference genome. Core-
481 genome SNPs (cgSNPs, sites presented in all genomes) outside of repetitive regions were
482 identified and a whole-sequence alignment of remaining 72 plasmids against the reference was
483 generated using Snippy. A neighbour-joining tree were generated from recombination-free
484 cgSNPs using pairwise SNP counts as distance metrics (namely, SNP distances) **(Figure S8)**.

485

486 Maximum-likelihood phylogenetic reconstruction from the whole-genome plasmid alignment
487 (which includes invariant sites, gaps, and masked regions) was performed using IQ-Tree
488 v1.6.12[66], with the best-fit model "HKY+F+R2" (determined through extended model
489 selection and full-tree search implemented in IQ-Tree), 10 independent runs (for tree selection),
490 and 500 bootstrap replicates (for branch supports). The resulting unrooted tree was corrected
491 for recombination using ClonalFrameML [67] with its default parameters and the whole-genome
492 alignment of plasmids. Major plasmid lineages were identified from topology of the corrected
493 tree. Detected recombination regions and reconstructed ancestral sequences were drawn against
494 the corrected tree using the script cfml_results.R from ClonalFrameML. Sample information
495 and AMR gene content of IMP isolates harbouring these plasmids were drawn against the
496 plasmid tree using iTOL v5[68]. The dating of internal nodes of the plasmid tree was inferred by
497 BactDating using the mixed-Gamma model, root-finding algorithm, 5×10^4 random walks of
498 Markov Chain Monte Carlo (MCMC), and accounting for recombination identified by
499 ClonalFrameML. To evaluate the robustness of tree reconstruction, a cgSNP tree was generated
500 by IQ-Tree (best-fit model: "TIM3e+ASC"; other parameters were the same as reconstructing
501 the whole-genome tree) and corrected for recombination using ClonalFrameML (with default
502 parameters). Tree comparisons (**Figures S9–S12**) were performed in R v3.6.3 with function
503 tanglegram in package dendextend[69].
504
505 *Patient contact network analysis*
506 Ward locations and timings were extracted from the Electronic Health Record (EHR) data for
507 *bla*$_{\text{IMP}}$CPE positive patients to establish patient movement history. Movement to other
508 locations for procedures during an inpatient episode, such as endoscopy, interventional
509 radiology or operating theatres, was not examined. To reveal potential transmission events
510 structure, a patient contact network was constructed from patient movement history, which
511 included information on when and where patients were on the same ward (for more details
512 please see Suppl. Methods). Time aggregated patient contacts were subsequently clustered to
513 reveal groups of patients more closely linked together using the Walktrap community detection
514 algorithm[70]. In this framework, contacts were also weighted by the duration of time spent
515 together across their hospital episode, capturing that the probability of transmission increases
516 with the amount of time two patients spend together[71]. Moreover, a temporal analysis of patient
517 interactions was performed over the time ordered sequence of contacts between patients[72] and
518 used to assess patient roles and position in transmission (for more details please see Suppl.
519 Methods).

For insights into the spatial distribution of *bla*$_{IMP}$CPE, a spatial network of ward/hospital network, connected by the same *bla*$_{IMP}$CPE patient movement was generated. From this spatial network, the following was calculated: total number of days patient has spent on each ward over the time before they were known to be colonised with *bla*$_{IMP}$CPE and infection prevention and control measures were taken (their infectious in-hospital period); network structure to determine ward/hospital spread of *bla*$_{IMP}$CPE; highly visited wards from patients of each specific genomic sub-cluster were also determined (using PageRank[73,74]) and contrasted for evidence of genomic localisation to hospital spaces. All network analysis and visualisation was completed in Python, R, and Cytoscape[75].

Data availability

Illumina reads and draft genome assemblies of 85 isolates were deposited in European Nucleotide Archive (ENA) under the BioProject accession PRJEB38818.

Ethics

This study was carried out in accordance with ethics reference 21/LO/0170 (279677), protocol 21HH6538 Investigation of epidemiological and pathogenic factors associated with infectious diseases.

Acknowledgements

We thank the staff of the diagnostic microbiology laboratory of North West London Pathology, for isolate collection and storage. We would also like to acknowledge the support of the Imperial College Healthcare Trust NIHR Biomedical Research Centre (BRC). The Imperial BRC Genomics Facility has provided resources and support that have contributed to the research results reported within this paper. The Imperial BRC Genomics Facility is supported by NIHR funding to the Imperial Biomedical Research Centre.

Funding

This work has been funded in part by faculty of medicine, Siriraj hospital, Mahidol university, Thailand (awarded to AB) and Medical Research Council Clinical Academic Research Fellowship scheme (awarded to FD, grant number MR/T005254/1).

AM is funded in part by a scholarship from the Medical Research Foundation National PhD Training Programme in Antimicrobial Resistance Research (MRF-145-0004-TPG-AVISO), the EPSRC Centre for Mathematics of Precision Healthcare (EP/N014529/)and through an National Institute for Health Research Senior Research Investigator Award. AM and MB acknowledge funding from EPSRC grant EP/N014529/1 to MB, supporting the EPSRC Centre for Mathematics of Precision Healthcare. AS is funded by a PhD studentship from the Medical Research Council Doctoral Training Award to Imperial College London (MR/N014103/1). AME acknowledges support from the National Institute for Health Research (NIHR) Imperial Biomedical Research Centre (BRC). EJ is an Imperial College Research Fellow, funded by Rosetrees Trust and the Stoneygate Trust (M683). HA was supported by the Imperial Health Charity. XD is supported by the NIHR Health Protection Research Unit in Genomics and Enabling Data. AL acknowledges funding from the National Institute for Health Research Health Protection Research Unit (NIHR HPRU) in Modelling Methodology at Imperial College London (grant HPRU-2012–10080) and the National Institute for Health Research (NIHR) Health Protection Research Unit in Healthcare Associated Infections and Antimicrobial Resistance at University of Oxford (NIHR200915) in partnership with UK Health Security Agency. AH is a National Institute for Health Research (NIHR) Senior Investigator. AH, FD, EJ, AB, YW, ME are affiliated with the National Institute for Health Research Health Protection Research Unit (NIHR HPRU) in Healthcare Associated Infections and Antimicrobial Resistance at Imperial College London in partnership with the UK Health Security Agency (previously PHE), in collaboration with, Imperial Healthcare Partners, University of Cambridge and University of Warwick. This report is independent research funded by the National Institute for Health Research. The views expressed in this publication are those of the author(s) and not necessarily those of the NHS, the National Institute for Health Research, the Department of Health and Social Care or the UK Health Security Agency.

Transparency declarations

JT holds some shares in Oxford Nanopore Technologies. All other authors have nothing to declare.

Author contributions

Conceptualization: FD, EJ, AH, MB, FB, XD, ME. Data curation: YW, BA, EJ, AM, FD, SM, AW, ME. Formal analysis: AB, AM, YW, FB, FD, EJ, AW, MB, AH, ME. Funding acquisition: AB, FD, AH, ME. Investigation: AB, YW, AM, HA, RP, AL, AA, JT, LM, KM-

C, AS, GL-M, JR-M. Methodology: FD, AM, AW, SM, YW, EJ, BA, XD, MB, JO, KH, ME, JT, MG. Project administration: FB, AH, FD, EJ. Resources: FD, AH, AE, HD, KH, JT. Supervision: FD, EJ, AH, MB. Validation: KH, JT, ME, HD, AW, SM. Visualization: AB, AM, YW, EJ, FD. Writing – original draft and further drafts: AB, AM, YW, EJ, FD, FB. Writing – review & editing: All authors.

References

1 Otter, J. A. *et al.* Counting the cost of an outbreak of carbapenemase-producing Enterobacteriaceae: an economic evaluation from a hospital perspective. *Clinical microbiology and infection : the official publication of the European Society of Clinical Microbiology and Infectious Diseases* **23**, 188-196, doi:10.1016/j.cmi.2016.10.005 (2017).

2 Doi, Y. Treatment Options for Carbapenem-resistant Gram-negative Bacterial Infections. *Clinical Infectious Diseases* **69**, S565-S575, doi:10.1093/cid/ciz830 (2019).

3 Pranita D. Tamma, S. L. A., Robert A. Bonomo, Amy J. Mathers, David van Duin, Cornelius J. Clancy. *Infectious Diseases Society of America Antimicrobial Resistant Treatment Guidance: Gram-Negative Bacterial Infections*, <https://www.idsociety.org/practice-guideline/amr-guidance/> (2020).

4 Branger, C. *et al.* Extended-spectrum β-lactamase-encoding genes are spreading on a wide range of Escherichia coli plasmids existing prior to the use of third-generation cephalosporins. *Microbial genomics* **4**, doi:10.1099/mgen.0.000203 (2018).

5 Li, X. *et al.* Diversification of broad host range plasmids correlates with the presence of antibiotic resistance genes. *FEMS microbiology ecology* **92**, doi:10.1093/femsec/fiv151 (2016).

6 Walsh, T. R., Toleman, M. A., Poirel, L. & Nordmann, P. Metallo-beta-lactamases: the quiet before the storm? *Clinical microbiology reviews* **18**, 306-325, doi:10.1128/cmr.18.2.306-325.2005 (2005).

7 Kananizadeh, P. *et al.* Emergence of carbapenem-resistant and colistin-susceptible Enterobacter cloacae complex co-harboring blaIMP-1 and mcr-9 in Japan.

8 Roberts, L. W. *et al.* Genomic analysis of carbapenemase-producing Enterobacteriaceae in Queensland reveals widespread transmission of bla IMP-4 on an IncHI2 plasmid. *Microbial genomics*, doi:10.1099/mgen.0.000321 (2019).

9 Matsumura, Y. *et al.* Global Molecular Epidemiology of IMP-Producing Enterobacteriaceae. *Antimicrobial agents and chemotherapy* **61**, doi:10.1128/aac.02729-16 (2017).

10 Turton, J. F. *et al.* IncN3 and IncHI2 plasmids with an In1763 integron carrying bla (IMP-1) in carbapenem-resistant Enterobacterales clinical isolates from the UK. *J Med Microbiol* **69**, 739-747, doi:10.1099/jmm.0.001193 (2020).

11 England, P. H. Vol. 15 *Health Protection report* 1-14 (Assets publishing service UK government, 2021).

12 Poirel, L., Jayol, A. & Nordmann, P. Polymyxins: Antibacterial Activity, Susceptibility Testing, and Resistance Mechanisms Encoded by Plasmids or Chromosomes. *Clinical microbiology reviews* **30**, 557-596, doi:10.1128/cmr.00064-16 (2017).

13 Ling, Z. *et al.* Epidemiology of mobile colistin resistance genes mcr-1 to mcr-9. *Journal of Antimicrobial Chemotherapy* **75**, 3087-3095, doi:10.1093/jac/dkaa205 (2020).

14 Liu, Y. Y. *et al.* Emergence of plasmid-mediated colistin resistance mechanism MCR-1 in animals and human beings in China: a microbiological and molecular biological study. *Lancet Infect Dis* **16**, 161-168, doi:10.1016/s1473-3099(15)00424-7 (2016).

15 Shen, Y. *et al.* Heterogeneous and Flexible Transmission of mcr-1 in Hospital-Associated Escherichia coli. *mBio* **9**, doi:10.1128/mBio.00943-18 (2018).

16 Carroll, L. M. *et al.* Identification of Novel Mobilized Colistin Resistance Gene mcr-9 in a Multidrug-Resistant, Colistin-Susceptible Salmonella enterica Serotype Typhimurium Isolate. *mBio* **10**, doi:10.1128/mBio.00853-19 (2019).

17 Osei Sekyere, J., Maningi, N. E., Modipane, L. & Mbelle, N. M. Emergence of *mcr*-9.1 in Extended-Spectrum-β-Lactamase-Producing Clinical Enterobacteriaceae in Pretoria, South Africa: Global Evolutionary Phylogenomics, Resistome, and Mobilome. *mSystems* **5** (2020).

18 Soliman, A. M. *et al.* Emergence of a Multidrug-Resistant Enterobacter hormaechei Clinical Isolate from Egypt Co-Harboring mcr-9 and bla(VIM-4). *Microorganisms* **8**, doi:10.3390/microorganisms8040595 (2020).

19 Macesic, N. *et al.* Silent spread of mobile colistin resistance gene mcr-9.1 on IncHI2 'superplasmids' in clinical carbapenem-resistant Enterobacterales. *Clinical Microbiology and Infection*, doi:https://doi.org/10.1016/j.cmi.2021.04.020 (2021).

20 Hendrickx, A. P. A. *et al.* A genetic cluster of MDR Enterobacter cloacae complex ST78 harbouring a plasmid containing blaVIM-1 and mcr-9 in the Netherlands. *JAC-Antimicrobial Resistance* **3**, doi:10.1093/jacamr/dlab046 (2021).

21 Li, Y. *et al.* Characterization of the global distribution and diversified plasmid reservoirs of the colistin resistance gene mcr-9. *Scientific Reports* **10**, 8113, doi:10.1038/s41598-020-65106-w (2020).

22 Meyers, L. Contact network epidemiology: Bond percolation applied to infectious disease prediction and control. *Bulletin of the American Mathematical Society* **44**, 63-86 (2006).

23 Newman, M. E. J. The Structure and Function of Complex Networks. *SIAM Review* **45**, 167-256, doi:10.1137/s003614450342480 (2003).

24 Pastor-Satorras, R., Castellano, C., Van Mieghem, P. & Vespignani, A. Epidemic processes in complex networks. *Reviews of Modern Physics* **87**, 925-979, doi:10.1103/RevModPhys.87.925 (2015).

25 Klovdahl, A. S. Social networks and the spread of infectious diseases: The AIDS example. *Social Science & Medicine* **21**, 1203-1216, doi:https://doi.org/10.1016/0277-9536(85)90269-2 (1985).

26 Keeling, M. J., Woolhouse, M. E. J., May, R. M., Davies, G. & Grenfell, B. T. Modelling vaccination strategies against foot-and-mouth disease. *Nature* **421**, 136-142, doi:10.1038/nature01343 (2003).

27 Salathé, M. *et al.* A high-resolution human contact network for infectious disease transmission. *Proceedings of the National Academy of Sciences* **107**, 22020-22025, doi:10.1073/pnas.1009094108 (2010).

28 Meyers, L. A., Newman, M. E. J. & Pourbohloul, B. Predicting epidemics on directed contact networks. *Journal of Theoretical Biology* **240**, 400-418, doi:https://doi.org/10.1016/j.jtbi.2005.10.004 (2006).

29 Ancel Meyers, L., Newman, M. E. J., Martin, M. & Schrag, S. Applying network theory to epidemics: control measures for Mycoplasma pneumoniae outbreaks. *Emerging infectious diseases* **9**, 204-210, doi:10.3201/eid0902.020188 (2003).

30 Newman, M. E. J. Spread of epidemic disease on networks. *Physical Review E* **66**, 016128, doi:10.1103/PhysRevE.66.016128 (2002).

31 Brockmann, D. & Helbing, D. The Hidden Geometry of Complex, Network-Driven Contagion Phenomena. *Science* **342**, 1337, doi:10.1126/science.1245200 (2013).

32 Colizza, V., Barrat, A., Barthélemy, M. & Vespignani, A. The role of the airline transportation network in the prediction and predictability of global epidemics. *Proceedings of the National Academy of Sciences* **103**, 2015-2020, doi:10.1073/pnas.0510525103 (2006).

683 33 Kwong, J. C. *et al.* Translating genomics into practice for real-time surveillance and response
684 to carbapenemase-producing Enterobacteriaceae: evidence from a complex multi-
685 institutional KPC outbreak. *PeerJ* **6**, e4210-e4210, doi:10.7717/peerj.4210 (2018).
686 34 Gouliouris, T. *et al.* Quantifying acquisition and transmission of Enterococcus faecium using
687 genomic surveillance. *Nat Microbiol*, doi:10.1038/s41564-020-00806-7 (2020).
688 35 Otter, J. A. *et al.* Detecting carbapenemase-producing Enterobacterales (CPE): an evaluation
689 of an enhanced CPE infection control and screening programme in acute care. *Journal of*
690 *Antimicrobial Chemotherapy* **75**, 2670-2676, doi:10.1093/jac/dkaa192 (2020).
691 36 Rodriguez-Manzano, J. *et al.* Rapid Detection of Mobilized Colistin Resistance using a Nucleic
692 Acid Based Lab-on-a-Chip Diagnostic System. *Scientific reports* **10**, 8448, doi:10.1038/s41598-
693 020-64612-1 (2020).
694 37 Furniss, R. C. D. *et al.* Detection of Colistin Resistance in <span class="named-content genus-
695 species" id="named-content-1">Escherichia coli by Use of the MALDI Biotyper Sirius
696 Mass Spectrometry System. *Journal of clinical microbiology* **57**, e01427-01419,
697 doi:10.1128/jcm.01427-19 (2019).
698 38 Landman, D., Salamera, J. & Quale, J. Irreproducible and uninterpretable Polymyxin B MICs for
699 Enterobacter cloacae and Enterobacter aerogenes. *Journal of clinical microbiology* **51**, 4106-
700 4111, doi:10.1128/jcm.02129-13 (2013).
701 39 Fournier, S. *et al.* Efficiency of different control measures for preventing carbapenemase-
702 producing enterobacteria and glycopeptide-resistant Enterococcus faecium outbreaks: a 6-
703 year prospective study in a French multihospital institution, January 2010 to December 2015.
704 *Euro Surveill* **23**, 17-00078, doi:10.2807/1560-7917.ES.2018.23.8.17-00078 (2018).
705 40 Haenni, M. *et al.* Co-occurrence of extended spectrum β lactamase and MCR-1 encoding genes
706 on plasmids. *Lancet Infect Dis* **16**, 281-282, doi:10.1016/s1473-3099(16)00007-4 (2016).
707 41 Yin, W. *et al.* Novel Plasmid-Mediated Colistin Resistance Gene mcr-3 in Escherichia coli. *MBio*
708 **8**, doi:10.1128/mBio.00543-17 (2017).
709 42 Kieffer, N. *et al.* mcr-9, an Inducible Gene Encoding an Acquired Phosphoethanolamine
710 Transferase in Escherichia coli, and Its Origin. *Antimicrobial agents and chemotherapy* **63**,
711 doi:10.1128/aac.00965-19 (2019).
712 43 Otter, J. A. *et al.* Emergence and clonal spread of colistin resistance due to multiple mutational
713 mechanisms in carbapenemase-producing Klebsiella pneumoniae in London. *Scientific reports*
714 **7**, 12711, doi:10.1038/s41598-017-12637-4 (2017).
715 44 Otter, J. A., Mutters, N. T., Tacconelli, E., Gikas, A. & Holmes, A. H. Controversies in guidelines
716 for the control of multidrug-resistant Gram-negative bacteria in EU countries. *Clinical*
717 *microbiology and infection : the official publication of the European Society of Clinical*
718 *Microbiology and Infectious Diseases* **21**, 1057-1066, doi:10.1016/j.cmi.2015.09.021 (2015).
719 45 Jamal, A. J. *et al.* Infection prevention and control practices related to carbapenemase-
720 producing Enterobacteriaceae (CPE) in acute-care hospitals in Ontario, Canada. *Infection*
721 *Control & Hospital Epidemiology* **40**, 1006-1012, doi:10.1017/ice.2019.173 (2019).
722 46 Harris, A. D., McGregor, J. C. & Furuno, J. P. What Infection Control Interventions Should Be
723 Undertaken to Control Multidrug-Resistant Gram-Negative Bacteria? *Clinical Infectious*
724 *Diseases* **43**, S57-S61, doi:10.1086/504479 (2006).
725 47 Doron, S. & Davidson, L. E. Antimicrobial stewardship. *Mayo Clin Proc* **86**, 1113-1123,
726 doi:10.4065/mcp.2011.0358 (2011).
727 48 Amoureux, L. *et al.* Nosocomial Infections with IMP-19-Producing Pseudomonas aeruginosa
728 Linked to Contaminated Sinks, France. *Emerging infectious diseases* **23**, 304-307,
729 doi:10.3201/eid2302.160649 (2017).
730 49 Mollenkopf, D. F. *et al.* Carbapenemase-Producing Enterobacteriaceae Recovered from the
731 Environment of a Swine Farrow-to-Finish Operation in the United States. *Antimicrobial agents*
732 *and chemotherapy* **61**, e01298-01216, doi:10.1128/AAC.01298-16 (2017).

50 Heireman, L. *et al.* Toilet drain water as a potential source of hospital room-to-room transmission of carbapenemase-producing Klebsiella pneumoniae. *The Journal of hospital infection* **106**, 232-239, doi:10.1016/j.jhin.2020.07.017 (2020).
51 Regev-Yochay, G. *et al.* Sink traps as the source of transmission of OXA-48-producing Serratia marcescens in an intensive care unit. *Infect Control Hosp Epidemiol* **39**, 1307-1315, doi:10.1017/ice.2018.235 (2018).
52 EUCAST. Breakpoint tables for interpretation of MICs and zone diameters. Version 7.1. *European Committee on Antimicrobial Susceptibility Testing* (2017).
53 Rodriguez-Manzano, J. *et al.* Rapid Detection of Mobilized Colistin Resistance using a Nucleic Acid Based Lab-on-a-Chip Diagnostic System. *Sci Rep* **10**, 8448, doi:10.1038/s41598-020-64612-1 (2020).
54 Andrews, S. FASTQC. A quality control tool for high throughput sequence data. (2010).
55 Bolger, A. M., Lohse, M. & Usadel, B. Trimmomatic: a flexible trimmer for Illumina sequence data. *Bioinformatics (Oxford, England)* **30**, 2114-2120, doi:10.1093/bioinformatics/btu170 (2014).
56 Bankevich, A. *et al.* SPAdes: A New Genome Assembly Algorithm and Its Applications to Single-Cell Sequencing. *Journal of Computational Biology* **19**, 455-477, doi:10.1089/cmb.2012.0021 (2012).
57 Seemann, T. Prokka: rapid prokaryotic genome annotation. *Bioinformatics* **30**, 2068-2069, doi:10.1093/bioinformatics/btu153 (2014).
58 Larsen, M. V. *et al.* Benchmarking of methods for genomic taxonomy. *Journal of clinical microbiology* **52**, 1529-1539, doi:10.1128/jcm.02981-13 (2014).
59 Larsen, M. V. *et al.* Multilocus sequence typing of total-genome-sequenced bacteria. *Journal of clinical microbiology* **50**, 1355-1361, doi:10.1128/jcm.06094-11 (2012).
60 Jolley, K. A., Bray, J. E. & Maiden, M. C. J. Open-access bacterial population genomics: BIGSdb software, the PubMLST.org website and their applications. *Wellcome Open Res* **3**, 124, doi:10.12688/wellcomeopenres.14826.1 (2018).
61 Zankari, E. *et al.* Identification of acquired antimicrobial resistance genes. *J Antimicrob Chemother* **67**, 2640-2644, doi:10.1093/jac/dks261 (2012).
62 Carattoli, A. *et al.* In silico detection and typing of plasmids using PlasmidFinder and plasmid multilocus sequence typing. *Antimicrobial agents and chemotherapy* **58**, 3895-3903, doi:10.1128/aac.02412-14 (2014).
63 Jain, C., Rodriguez, R. L., Phillippy, A. M., Konstantinidis, K. T. & Aluru, S. High throughput ANI analysis of 90K prokaryotic genomes reveals clear species boundaries. *Nature communications* **9**, 5114, doi:10.1038/s41467-018-07641-9 (2018).
64 Gilmour, M. W., Thomson, N. R., Sanders, M., Parkhill, J. & Taylor, D. E. The complete nucleotide sequence of the resistance plasmid R478: defining the backbone components of incompatibility group H conjugative plasmids through comparative genomics. *Plasmid* **52**, 182-202, doi:https://doi.org/10.1016/j.plasmid.2004.06.006 (2004).
65 Kurtz, S. *et al.* Versatile and open software for comparing large genomes. *Genome Biology* **5**, R12, doi:10.1186/gb-2004-5-2-r12 (2004).
66 Nguyen, L.-T., Schmidt, H. A., von Haeseler, A. & Minh, B. Q. IQ-TREE: A Fast and Effective Stochastic Algorithm for Estimating Maximum-Likelihood Phylogenies. *Molecular Biology and Evolution* **32**, 268-274, doi:10.1093/molbev/msu300 (2014).
67 Didelot, X. & Wilson, D. J. ClonalFrameML: efficient inference of recombination in whole bacterial genomes. *PLoS computational biology* **11**, e1004041, doi:10.1371/journal.pcbi.1004041 (2015).
68 Letunic, I. & Bork, P. Interactive Tree Of Life (iTOL): an online tool for phylogenetic tree display and annotation. *Bioinformatics (Oxford, England)* **23**, 127-128, doi:10.1093/bioinformatics/btl529 (2006).

69 Galili, T. dendextend: an R package for visualizing, adjusting and comparing trees of hierarchical clustering. *Bioinformatics (Oxford, England)* **31**, 3718-3720, doi:10.1093/bioinformatics/btv428 (2015).

70 Pons, P. & Latapy, M. 284-293 (Springer Berlin Heidelberg).

71 Gómez, S., Arenas, A., Borge-Holthoefer, J., Meloni, S. & Moreno, Y. Discrete-time Markov chain approach to contact-based disease spreading in complex networks. *EPL (Europhysics Letters)* **89**, 38009, doi:10.1209/0295-5075/89/38009 (2010).

72 Holme, P. & Saramäki, J. Temporal networks. *Physics Reports* **519**, 97-125, doi:https://doi.org/10.1016/j.physrep.2012.03.001 (2012).

73 Senanayake, U., Piraveenan, M. & Zomaya, A. The Pagerank-Index: Going beyond Citation Counts in Quantifying Scientific Impact of Researchers. *PloS one* **10**, e0134794-e0134794, doi:10.1371/journal.pone.0134794 (2015).

74 Page, L., Brin, Sergey, Motwani, Rajeev, Winograd, Terry. The PageRank Citation Ranking: Bringing Order to the Web. (Stanford University, Stanford InfoLab Publication Server, 1999).

75 Shannon, P. *et al.* Cytoscape: a software environment for integrated models of biomolecular interaction networks. *Genome Res* **13**, 2498-2504, doi:10.1101/gr.1239303 (2003).